Environ Dev Sustain (2017) 19:2475–2485
DOI 10.1007/s10668-016-9866-8

Modeling of high step-up converter in closed loop for renewable energy applications

R. Nagaraj[1] · D. Thiruganamurthy[2] · Manik Murthy Rajput[1]

Received: 23 July 2015 / Accepted: 29 September 2016 / Published online: 6 October 2016

Abstract A majority of small-scale renewable energy sources including the solar PV modules, fuel cells gives out output voltage in the range of around 15–40 V DC. This needs to be stepped up to suit load requirements using a high voltage gain converter. Since renewable sources inherently generate sudden variations in input voltage, a good output voltage profile even during such random variations in input conditions is essential. This paper presents modeling of a high step-up converter configuration with closed loop control. The converter topology is designed to operate with moderate duty ratios and the simple coupled inductor. The converter is capable of high step-up and can find application in solar PV systems. The controller response is good with low steady state error and required dynamics. The modeling and simulation is carried out using MATLAB/Simulink software package.

Keywords PV module · Coupled inductor · Single switch · DC–DC power convertors · PI controller

1 Introduction

The power electronic technology plays a vital role in distributed generation and in integration of renewable energy sources into the electrical grid, and it is widely used and rapidly expanding as these applications become more integrated with the grid-based systems (Farmad and Biglar 2012) The increasing number of renewable energy sources and

✉ R. Nagaraj
rnagaraj@igcar.gov.in

D. Thiruganamurthy
dtm@igcar.gov.in

Manik Murthy Rajput
manik@igcar.gov.in

1 NDDP, BARC Facilities, Kalpakkam 603 102, India

2 EID, IGCAR, Kalpakkam 603 102, India

distributed generators requires new strategies for the operation and management of the electricity grid in order to maintain or even to improve the power supply reliability and quality (Oyedepo et al. 2014). In addition, liberalization of the grids leads to new management structures, in which trading of energy and power is becoming increasingly important (Sagar and Goel 2014).

Solar panels have now become an important alternate source for the power generation. The scale of production is expected to reach to tens of gigawatt in the future. Solar photovoltaic (PV) system has got obvious advantages when compared to other renewable energy systems as this is silent, modular, easily transportable and quickly installed. Power can be generated in situ eliminating the need of long transmission lines. Also, small-scale systems like terrestrial applications of photovoltaic panels supplement the other conventional power generation (Rodriguez and Amaratunga 2008). An ac module is a micro-inverter configured on the rear bezel of a PV panel (Shimizu et al. 2006; Kjaer et al. 2005); this alternative solution not only immunizes against the yield loss by shadow effect, but also provides flexible installation options in accordance with the user's budget (Umeno et al. 1991).

The required level of DC voltage can be obtained by connecting a series of PV panels. But this solution may not be suitable for low power applications where putting more PV devices will end up in higher capacities and also occupy large space making this option unviable. Also high voltage generated from PV panels can be a safety issue in low power applications. Hence there is a serious need for efficient power electronic conversion systems for low power applications of the order of 100 W. The possible applications include low power domestic solar PV system with less than a couple of PV panels generating less than 40 V DC and require to be stepped up for use in domestic appliances. Also it can be used in integrated and compact mobile power units with possible applications in powering up of mobile devices, LED lamps and low mechanical power applications like pumping water and small desalination plant systems (Garcia-Valverde et al. 2016; Nagaraj et al. 2016; Nagaraj 2012; Nagaraj and Panigrahi 2015).

In this paper presented a DC–DC converter with coupled inductor in open loop and closed loop operation during critical loading condition is proposed. The main concept is to obtain high step-up voltage from low voltage delivering devices like photovoltaic panels. Furthermore, a general conceptual circuit for high step-up, low-cost, and high efficiency dc/dc conversion is proposed to derive the next generation topologies for the PV connected system.

The range of power capacity for a single PV panel (Shimizu et al. 2006; Kjaer et al. 2005) is about 100 to 300 W, and the maximum power point (MPP) voltage range is about 15 to 40 V, which will be the input voltage of the ac module; in cases with lower input voltage, it is difficult for the ac module to reach high efficiency (Kjaer et al. 2005). However, by employing a high step-up dc–dc converter (Zhao and Lee 2003; Chen et al. 2012) in the front of the inverter improves power conversion efficiency and provides a stable dc link to the inverter. When installing the PV generation system during daylight, for safety reasons, the ac module outputs zero voltage.

2 Description and modeling of the high step-up converter

Figure 1 shows the general power generation system with a high step-up converter. When installation of the ac module is taking place, this potential difference could pose the hazards to both the worker and the facilities. A floating active switch is designed and

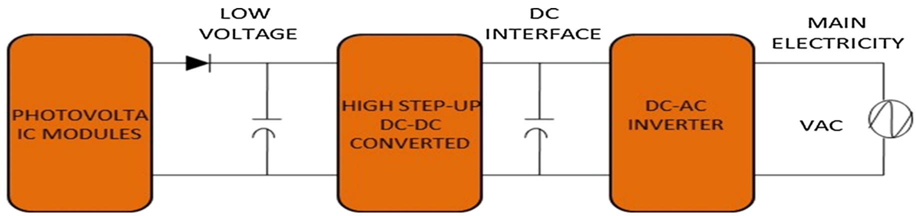

Fig. 1 Schematic PV generation system with a high step-up converter

placed in series to isolate the dc current from the PV panel, for when the ac module is off-grid as well as in non-operating condition. This isolation ensures the operation of the internal components without any energy being transferred to the output or input terminals, which could be unsafe.

The dc–dc converter requires large step-up conversion (Zhao and Lee 2003; Chen et al. 2012) from the panel's low voltage to the voltage level of the application. The efficiency and voltage gain of the dc–dc boost converter are constrained by either the parasitic effect of the power switches or the reverse recovery issue of the diodes. In addition, the equivalent series resistance (ESR) of the capacitor and the parasitic resistances of the inductor also affect overall efficiency (Chen et al. 2011).

The converter shown in Fig. 2 gives a large step-up voltage conversion ratio because of the connection of the two pairs of inductors, capacitor, and diode. The energy of the inductor is recycled through the freewheeling diodes $D1$ and $D2$ to increase efficiency (Zhao and Lee 2003).

Under steady state, the input voltage Vin is applied across $N1$ winding of coupled inductor. This induces a voltage of n times of Vin with polarity as shown in Fig. 3 where n is the turns ratio of coupled inductor. Two circulating currents ic1 and ic2 are setup in the loops in directions shown in Fig. 3. The voltage across the capacitors V_{c1}, V_{c2} are also setup due to these currents. These voltages have the polarity as per the respective current directions, and it can be seen that they are in such a way to aid the incoming voltage.

From Fig. 3, the output voltage V_o is the sum of voltage drops across the capacitors $C1$/$C2$ (V_{c1}/V_{c2}) and the coupled inductors N_1/N_2 (V_{n1}/V_{n2}) with the input voltage V_{in} (Axelrod et al. 2008; Liang et al. 2012; Yang and Liang 2012). This is given by Eq. (1).

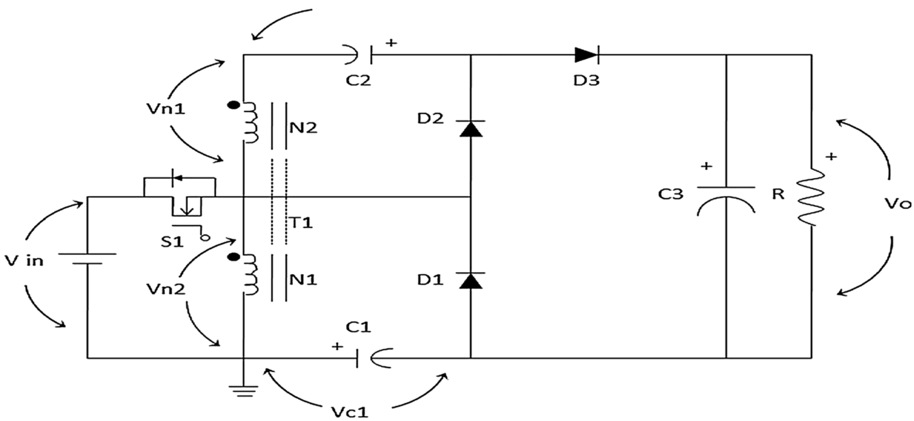

Fig. 2 Circuit configuration of high step-up converter

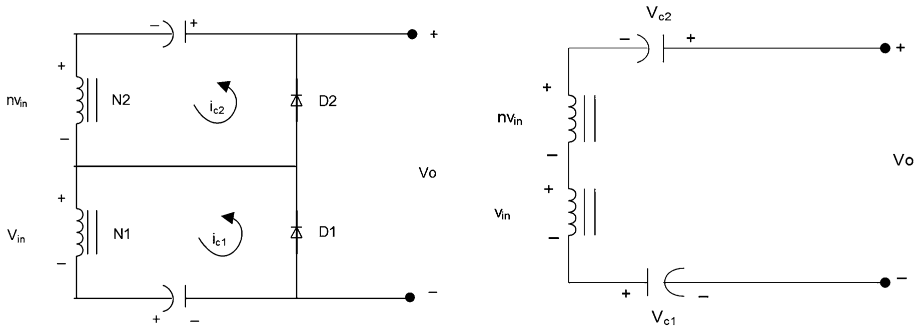

Fig. 3 *Diagram* indicating the current and voltage polarities under steady state

$$V_0 = V_{\text{in}} + V_{n2} + V_{C2} + V_{C1} \tag{1}$$

The voltage across capacitors C_1 and C_2 is obtained as follows:

$$V_{C1} = \frac{D}{1 - D} V_{\text{in}} \tag{2}$$

$$V_{C2} = \frac{nD}{1 - D} V_{\text{in}} \tag{3}$$

where D is the duty cycle and n is the turns ratio of the coupled inductor T_1 windings which is equal to N_2/N_1.

Substituting Eqs. 2 and 3 in Eq. 1, we get

$$V_0 = V_{\text{in}} + nV_{\text{in}} + \frac{nD}{1 - D} V_{\text{in}} + \frac{D}{1 - D} V_{\text{in}} \tag{4}$$

The overall voltage gain M is as follows:

$$M = \frac{V_0}{V_{\text{in}}} = \frac{1 + n}{1 - D} \tag{5}$$

To select the turns ratio of the coupled inductor, we have plotted the voltage gain against the duty ratios for various values of turns ratio using Eq. 5. The obtained plot is shown in Fig. 4.

From the plot, we can see that with moderate duty ratios in the range of 0.4 to 0.6 and switching frequency $f_s = 50$ kHz, we are able to obtain the voltage gain in the range of 8 to 17. We have chosen the turns ratio of $n = 5$. Hence, for $V_{\text{in}} = 15$ V and $V_o = 200$ V, we need a turns ratio close to 13 which is obtainable at duty ratio of 0.55. The capacitor $C1$ and $C2$ are selected as 47 μF, and their equivalent series resistance (ESR) values are chosen as 4.203 Ohms from capacitor data sheet. The output capacitor $C3$ is chosen as 220 μF. The converter is designed for 100 W, and hence the maximum load is also designed for 100 W. Hence, at an output voltage of 200 V, the load resistor chosen is 400 Ohms.

Considering the efficiency of 80 % under worst case for design considerations with minimum input voltage of $V_{\text{in}} = 15$ V, the input power is 125 W and input current I_{in} is 8.33 A for the rated output power of 100 W.

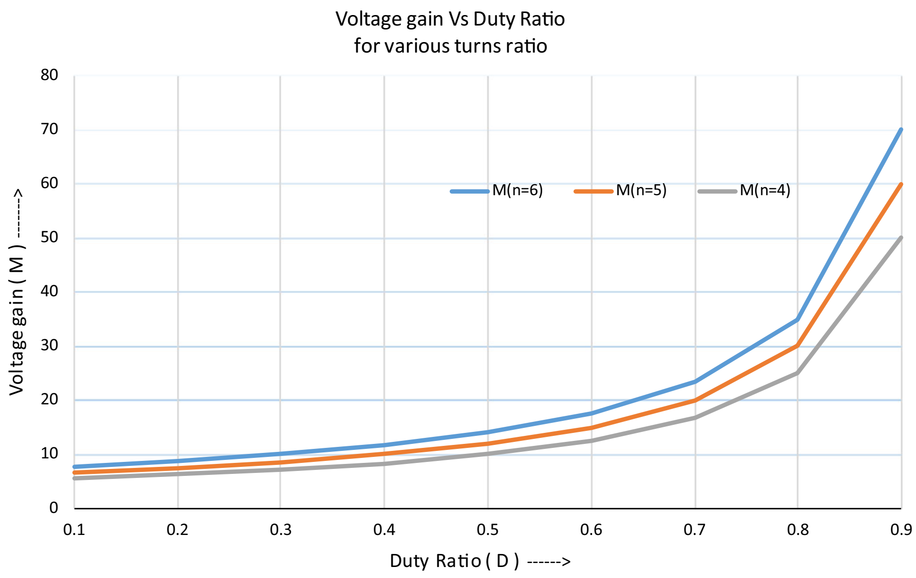

Fig. 4 Voltage gain for various duty ratios with different values of n

The magnetizing inductance L_{m} of the coupled inductor

$$L_{\mathrm{m}} > \frac{DV_{\mathrm{in}}T_s}{I_{\mathrm{in}}} > 21.6\ \mu\mathrm{H} \tag{6}$$

where $T_s = 1/f$s.

We have chosen the magnetizing inductance L_m to be 30 µH.

With the usage of power electronics technology controls any load conditions with certain parameters. For getting constant load achieving condition, we need to go for closed loop operation with the help of second-order compensators such as P, PI, PID controllers with respect to maintain constant voltage at load.

Here, PI controller is used as shown in Fig. 4, because of its fast dynamic response with respect to steady state error $e_{\mathrm{rr}} \approx 0$, without any load changes. In this, the V_{act} and V_{ref} are compared, with respect to these changes the switching operation depends on the reference signal coming from proposed controller, compare reference signal with carrier (saw tooth) for generation of pulses with respect to load changes, with the help of pulse converter actuates and maintain constant output voltage and achieve load condition (Fig. 5).

3 Results: MATLAB modeling and simulation

The converter is modeled in MATLAB/Simulink to analyze and study the performance of the system. Figure 6 shows the MATLAB/Simulink model of high step-up DC–DC converter using PI controller. Figure 7 shows the step response and Bode plot for the converter in closed loop.

The open loop transfer function of the above system is obtained from Eq. (4) and is as given below:

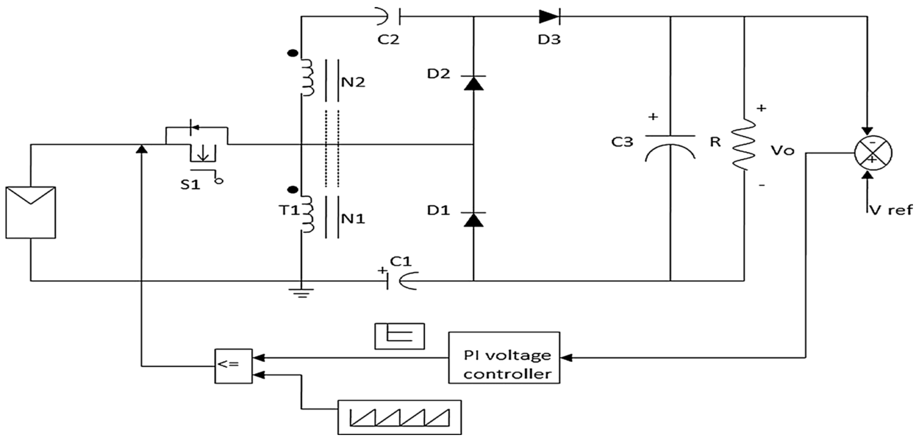

Fig. 5 High step-up dc–dc converter PV system in closed loop with PI controller

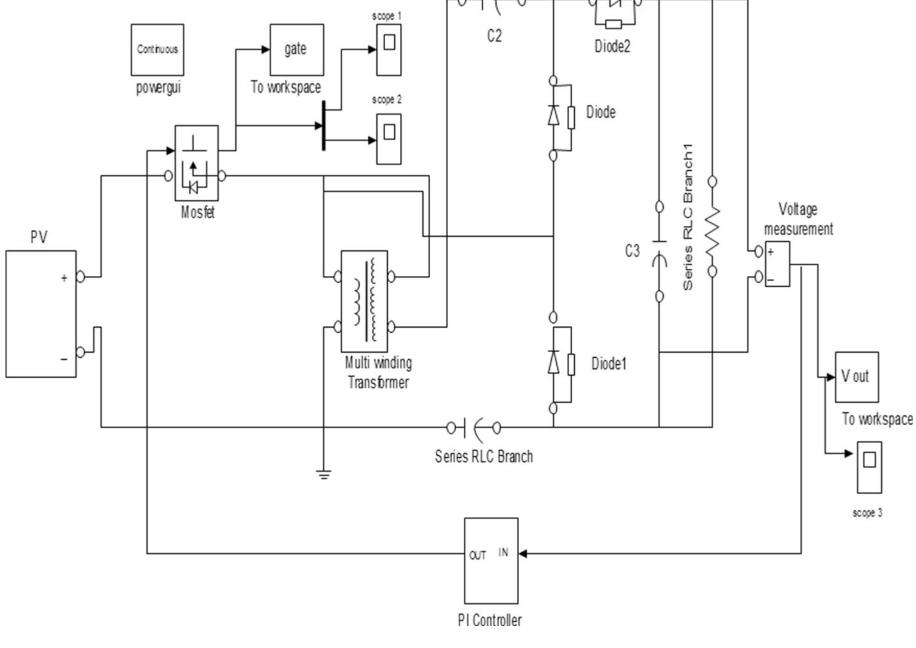

Fig. 6 *MATLAB*/Simulink of high step-up DC–DC converter using PI controller using *MATLAB*/Simulink

$$G(s) = \frac{V_o(s)}{V_{\text{in}}(s)} = I + n + \left(\frac{D}{I - D}\right) \cdot \frac{1}{SC_1} + \left(\frac{nD}{I - D}\right) \cdot \frac{1}{SC_2} \quad (7)$$

$$G(s) = \frac{[(1+n)(1-D)C_1C_2]S^2 + (C_1 + C_2)S}{(1-D)S^2C_1C_2} \quad (8)$$

With PI controller in the feedback loop, the feedback loop transfer function is given by

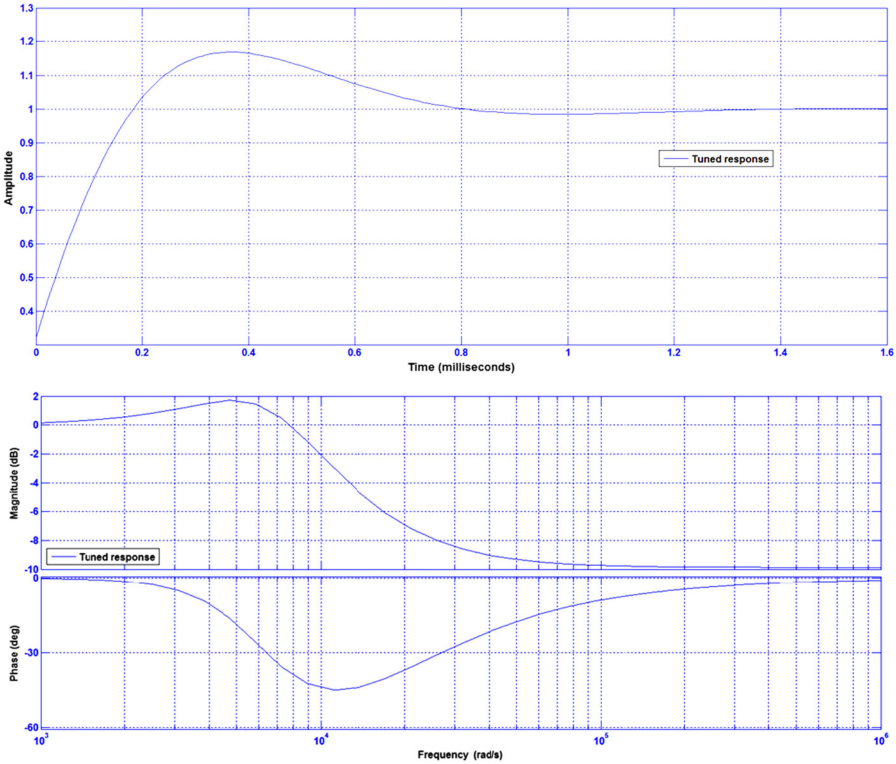

Fig. 7 Step response and bode plot for the converter in closed loop

$$H(s) = K_p + \frac{K_i}{S} \tag{9}$$

Then, the overall closed loop transfer function is given by

$$T.F = \frac{G(s)}{1 + G(s) \cdot H(s)} \tag{10}$$

The above models Eqs. (7)–(10) were implemented in MATLAB. Tuning of the PI was performed during the Simulink environment by loading the transfer function model of the overall system.

The controller was tuned initially by increasing the K_p value till oscillations are set. Then, K_i value was increased to obtain steady state with minimum error. The K_p and K_i values were set to 9.1 and 1.7, respectively. We obtained the stable performance with <17 % peak overshoot and rise time of <0.2 ms.

The output voltage and current waveforms of capacitors and diodes are shown in Figs. 8 and 9. This shows that there is no extreme voltage stress across the components and high current through the components (Fig. 10).

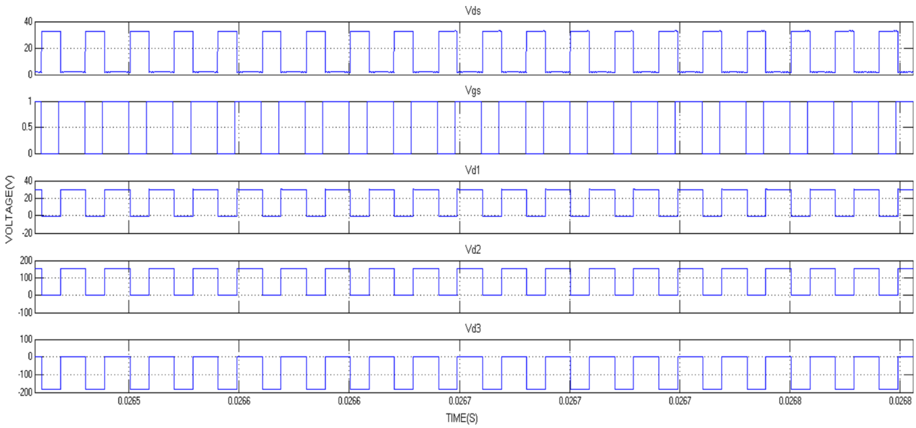

Fig. 8 Output voltage waveforms of capacitors and diodes of high step-up DC–DC converter using PI controller

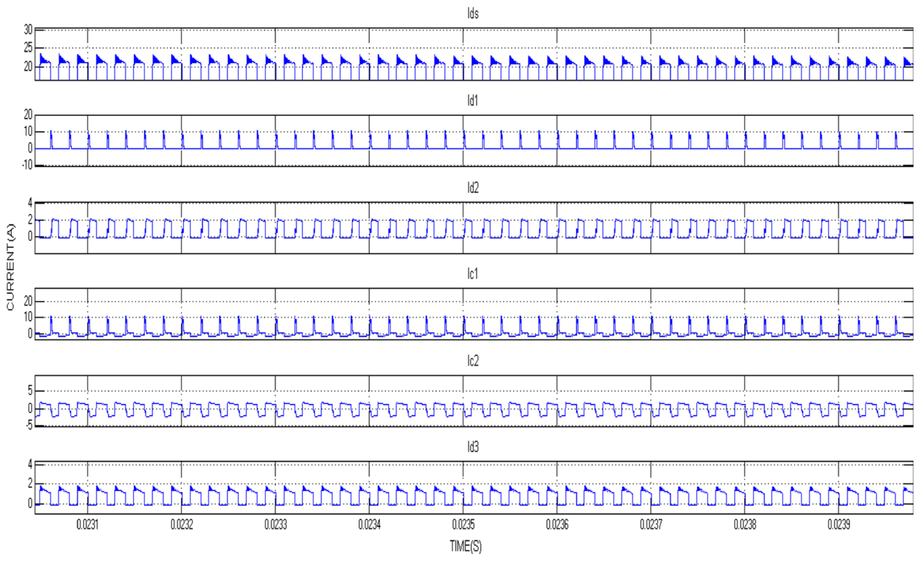

Fig. 9 Output current waveforms of capacitors and diodes of high step-up DC–DC converter using PI controller

4 Performance with variation in input voltage

The system was subjected to variation in input voltage to observe variation in output voltage to verify the response of the converter in closed loop. First, the converter was given with an input voltage that varies every 0.1 s within the range of 15 to 40 V. The input and output voltage waveforms are as shown in Fig. 11. We observe that after initial oscillation with maximum of around 5 %, the output voltage settles down and further steady voltage variations does not affect the output voltage to great extent and gives a near-straight line performance.

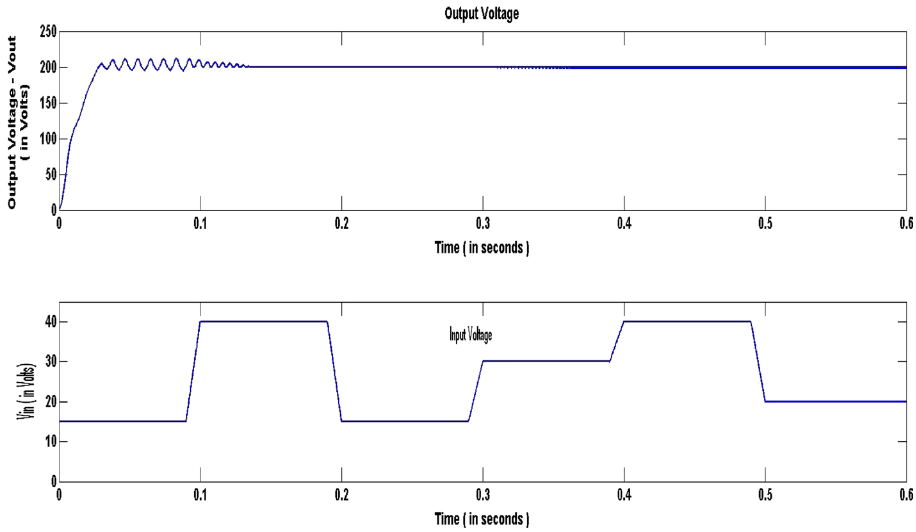

Fig. 10 Output voltage response for steady change in input voltage

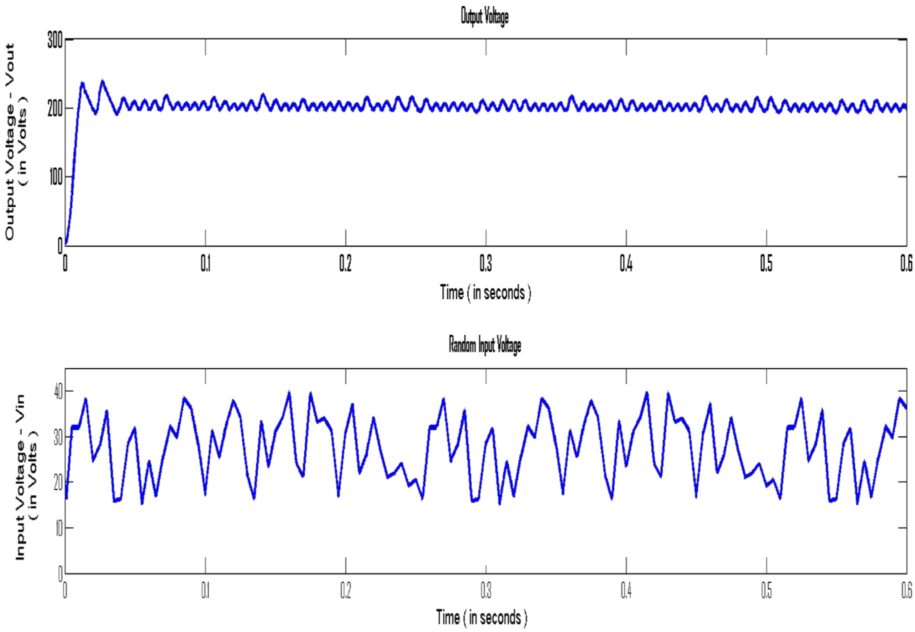

Fig. 11 Output voltage response for random input voltage

Further to verify the converter for application in renewable energy systems where variations of input voltage can be very much random based on solar irradiations, cloud movement etc., we generated a random voltage waveform that varies much faster in fraction of second within the range of 15 to 40 V. This input voltage waveform was used to evaluate the performance of converter, and the same is given in Fig. 11. Under such harsh input voltage conditions also, the output voltage could be controlled easily within the band of ±5 %. We can observe response of the controller with slight overshoots for sudden rise or drop in input voltage and the oscillations damping in two or three cycles.

5 Conclusion

Renewable energy resources (RES) are being increasingly applications to many more systems with help of power electronic conversion technology; by using this technology, we achieve high reliability to support the grid-connected system as well as standalone system. Here, we proposed a 100-W high step-up dc–dc converter with closed loop combination for attaining the constant load condition with respect to time with input voltage of 15 to 40 V range and output voltage of 200 V. The performance of the system was modeled in MATLAB/Simulink to study the behavior of the system. The closed loop transfer function of the system was derived. The step response and bode plot gave satisfactory performance with peak overshoot of <17 % and rise time of less than 0.2 ms, and the system was stable. The controller performance for steady and random input voltage variations was also studied, and satisfactory performance was observed. Thus, the converter in closed loop achieves high step-up voltage gain in the range of 8–13 times of input voltage, and the high performance of closed loop operation provides better results with better steady state error and fast dynamic response. Hence, the proposed configuration is suitable for application in low power devices for renewable sources-based systems that are subjected to large and random variations in input voltages.

References

Axelrod, B., Berkovich, Y., & Ioinovici, A. (2008). Switched-capacitor/switched-inductor structures for getting transformerless hybrid dc–dc PWM converters. *IEEE Transactions on Circuits and Systems I: Regular Papers, 55*(2), 687–696.

Chen, S. M., Liang, T. J., Yang, L. S., & Chen, J. F. (2011). A cascaded high step-up dc–dc converter with single switch for micro source applications. *IEEE Transactions on Power Electronics, 26*(4), 1146–1153.

Chen, S.-M., Liang, T.-J., Yang, L.-S., & Chen, J.-F. (2012). A safety enhanced, high step-up DC–DC converter for AC photovoltaic module application. *IEEE Transactions on Power Electronics, 27*(4), 1809–1817.

Farmad, H. S., & Biglar, S. (2012). Integration of demand side management, distributed generation, renewable energy sources and energy storages. *Integration of renewables into the distribution grid, CIRED 2012 workshop* (Vol. 1, No. 4, pp. 29–30). doi:10.1049/cp.2012.0784.

Garcia-Valverde, R., Villarejo, J. A., Hösel, M., Madsen, M. V., Søndergaard, R. R., Jørgensen, M., et al. (2016). Scalable single point power extraction for compact mobile and stand-alone solar harvesting power sources based on fully printed organic photovoltaic modules and efficient high voltage DC/DC conversion. *Solar Energy Materials and Solar Cells, 144*, 48–54, ISSN 0927-0248. doi:10.1016/j.solmat.2015.08.020. (http://www.sciencedirect.com/science/article/pii/S0927024815004146).

Kjaer, S. B., Pedersen, J. K., & Blaabjerg, F. (2005). A review of single-phase grid-connected inverters for photovoltaic modules. *IEEE Transactions on Industry Applications, 41*(5), 1292–1306.

Liang, T.-J., Chen, S.-M., Yang, L.-S., Chen, J.-F., & Ioinovici, A. (2012). Ultra-large gain step-up switched-capacitor DC–DC converter with coupled inductor for alternative sources of energy. *IEEE Transactions on Circuits and Systems I: Regular Papers, 59*(4), 864–874. doi:10.1109/TCSI.2011.2169886.

Nagaraj, R. (2012). Renewable energy based small hybrid power system for desalination applications in remote locations. In *India international conference on power electronics, IICPE.*

Nagaraj, R., & Panigrahi, B. K. (2015). Simulation and hardware implementation of FPGA based controller for hybrid power system. *International Journal of Electrical Energy, 3*(2), 86–93.

Nagaraj, R., et al. (2016). Techno-economic analysis of hybrid power system sizing applied to small desalination plants for sustainable operation. *International Journal of Sustainable Built Environment*. doi:10.1016/j.ijsbe.2016.05.

Oyedepo, S. O., Agbetuyi, A. F., & Odunfa, M. K. (2014). Transmission network enhancement with renewable energy. *Journal of Fundamentals of Renewable Energy and Applications, 5*, 145. doi:10.4172/2090-4541.1000145.

Rodriguez, C., & Amaratunga, G. A. J. (2008). Long-lifetime power inverter for photovoltaic ac modules. *IEEE Transactions on Industrial Electronics, 55*(7), 2593–2601.

Sagar, E., & Goel, R. (2014). Large scale grid amalgamation of renewable energy sources in indian power system. *International Journal for Research & Development in Technology, 2*(3), 1–4.

Shimizu, T., Wada, K., & Nakamura, N. (2006). Flyback-type single-phase utility interactive inverter with power pulsation decoupling on the dc input for an ac photovoltaic module system. *IEEE Transactions on Power Electronics, 21*(5), 1264–1272.

Umeno, T, Takahashi, K., Ueno, F., Inoue, T., & Oota, I. (1991). A new approach to low ripple-noise switching converters on the basis of switched-capacitor converters. In *Proceedings of the IEEE International Symposium on Circuits and Systems,* pp. 1077–1080.

Yang, L. S., & Liang, T. J. (2012). Analysis and implementation of a novel bidirectional dc–dc converter. *IEEE Transactions on Industrial Electronics, 59*(1), 422–434.

Zhao, Q., & Lee, F. C. (2003). High-efficiency, high step-up dc–dc converters. *IEEE Transactions on Power Electronics, 18*(1), 65–73.